

Thermo mechanical analysis of the gas turbine blade

Ganesh*, K. N. Pandey, Devendra Pratap Singh

Mechanical Engineering Department, Motilal Nehru National Institute of Technology Allahabad, Prayagraj, U.P, India

Presented in International Conference on Advancements and Futuristic Trends in Mechanical and Materials Engineering held at Indian Institute of Technology Ropar (IITR), Rupnagar, during December 5-7, 2019.

ABSTRACT

KEYWORDS

Gas Turbine Blade,
CATIA,
CMSX-4,
CFD,
Presser and Temperature,
FEA,
Abaqus.

Gas turbine engines are extensively used in aerospace and power generation plants. In the gas turbine engine, the turbine blade is one of the most vital components. It is subjected to very complex loading conditions at high temperature along with high centrifugal and pressure load. The performance and life of the gas turbine engine mostly depends on the gas turbine blades. In this study, a single crystal Ni-based superalloy (CMSX-4) is used as the material of a twisted gas turbine blade. Two different models of gas turbine blades have been created. One of those is uncooled blade and other is blade with cooling channels of constant cross-section along the span length. Both the models have been used for steady state CFD analysis to get temperature, pressure, and heat transfer coefficient distribution on the blade surface. From CFD results, transient heat transfer analysis was performed to get temperature distribution in the blade. The temperature distribution obtained from heat transfer analysis along with centrifugal and pressure load is considered for transient thermo-mechanical analysis of the blade. In transient thermo-mechanical analysis maximum stress for model 1 and model 2 is 399.2 MPa and 380.8 MPa respectively.

1. Introduction

A gas turbine engine is a device that is designed to convert the thermal energy of a fuel into some form of useful power, such as mechanical (or shaft) power or a high-speed thrust of a jet. Today, gas turbines (GTs) are widely used in aircraft propulsion, land-based power generation, and other industrial applications. Gas turbines works on both open and closed Brayton cycle. Gas turbines consist of a rotating compressor then a combustion chamber and then a rotating turbine to extract the work from compressed gas. In turbine engine turbine shaft is coupled with the compressor to drive the compressor. In open cycle gas turbines working fluid used is air which gets compressed up to high pressure in compressor then energy is added in to the compressed air in combustion chamber by igniting the fuel then this high pressure, high temperature air is passes through the turbine where it expands to exhaust pressure and produces the work output [1]. The systematic view of gas turbine components is shown in Fig. 1.

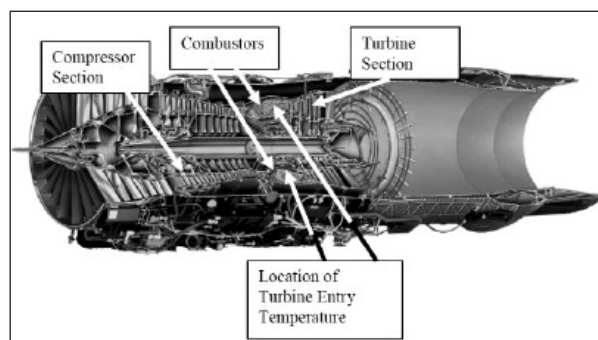


Fig. 1. Schematic diagram of gas turbine engine.

Thermo-mechanical fatigue is defined as a fatigue damage process under simultaneous changes in temperature and mechanical strains. Mechanical strains developed due to mechanical loading and additional thermal strains developed due to the cyclic thermal loading. Two major TMF cycles have been identified based on the phase difference between the temperature and total strain.

(i) In-phase TMF cycles (ii) Out-of-phase TMF cycles. [1, 4]. The Fig. 2 depicts about in-phase and out of phase behavior of Thermo mechanical Fatigue.

*Corresponding author,
E-mail: gk8726269298@gmail.com

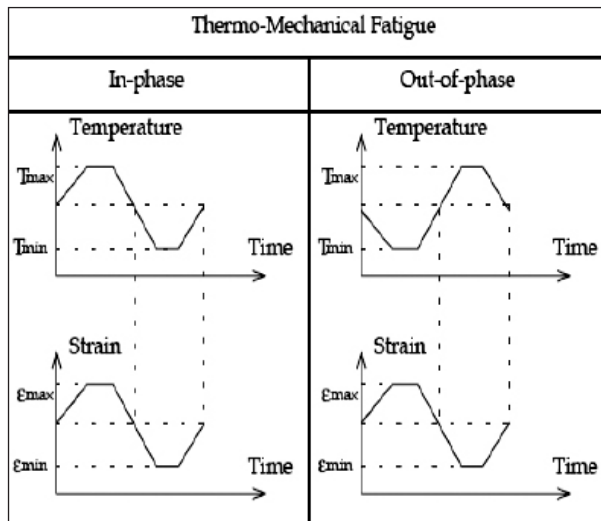


Fig. 2. In-phase and out of phase TMF cycles. [5].

Table 1

Cooling channels diameter for model 2.

Name of cooling channels	Diameter of cooling channels (mm)
Cooling Channel 1	5.550
Cooling Channel 2	4.887
Cooling Channel 3	4.164
Cooling Channel 4	3.702
Cooling Channel 5	3.200
Cooling Channel 6	2.537
Cooling Channel 7	1.749
Cooling Channel 8	1.042

2. Modelling of the Gas Turbine Blade

- Model 1 is an uncooled blade.
- Model 2 is a cooled blade with a constant cross-section of cooling channels.

The model 1 and model 2 are shown in Fig. 3.

In model 2 the diameters of cooling channels are given in Table1. The numbering of cooling channels has been done from leading edge to trailing edge as cooling 1 to cooling 8.

For modelling of cooling channels, cooling holes are created at 5 different cross-sections at different span length of the blade and then these holes are joined by multi section solid command. For validation of the modeling and computational technique employed for twisted blade, a C3X blade [6,7] of stainless steel was considered. The methodology adopted in the

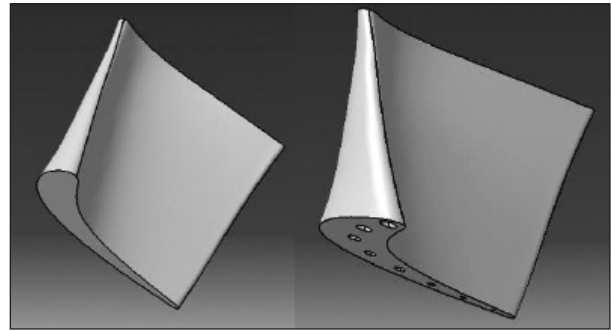


Fig. 3. Gas turbine blade model 1 (without cooling channel) and model 2 (with cooling channel).

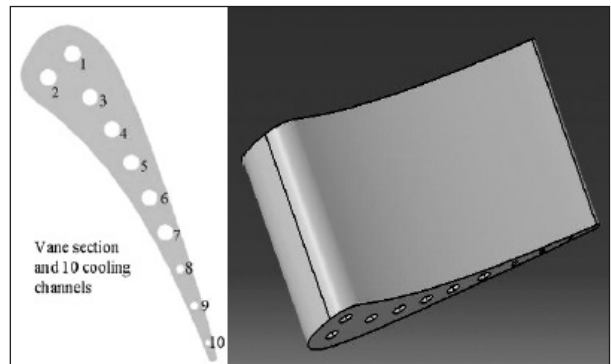


Fig. 4. Cross-section and solid model of C3X gas turbine blade. [6, 7].

Table 2

Cooling Channels Diameter for C3X Blade.

Cooling Channel	Diameter (mm)
Cooling Channel 1	6.30
Cooling Channel 2	6.30
Cooling Channel 3	6.30
Cooling Channel 4	6.30
Cooling Channel 5	6.30
Cooling Channel 6	6.30
Cooling Channel 7	6.30
Cooling Channel 8	3.10
Cooling Channel 9	3.10
Cooling Channel 10	1.98

present work is also verified from an experimental study on C3X blade [7]. This C3X blade consists of 10 cooling channels of constant diameters throughout the span length. The cross section and solid model of C3X gas turbine blade is shown in Fig. 4. In this experimental work a steady blade was used, and heat transfer effect of flowing fluid was studied. The height of C3X blade was 76.2 mm. The details of C3X blade data is given in Table 2.

3. Numerical Simulation

3.1 Steady state CFD analysis

CFD analysis is performed in the ANSYS CFX module of ANSYS 16.0.

The governing equations that used in CFD analysis are basically Navier stokes equations as given by equations (1) to (6).

3.11 Conservation of mass equation

$$\frac{\partial \bar{u}}{\partial x} + \frac{\partial \bar{v}}{\partial y} + \frac{\partial \bar{w}}{\partial z} = 0 \quad (1)$$

3.12 Conservation of linear momentum equation

X- Component

$$\rho \left(\bar{u} \frac{\partial \bar{u}}{\partial x} + \bar{v} \frac{\partial \bar{u}}{\partial y} + \bar{w} \frac{\partial \bar{u}}{\partial z} \right) = -\frac{\partial \rho}{\partial x} + \mu \nabla^2 \bar{u} - \frac{\partial}{\partial x} \rho \bar{u}'^2 - \frac{\partial}{\partial y} \rho \bar{u}' \bar{v}' - \frac{\partial}{\partial z} \rho \bar{u}' \bar{w}' \quad (2)$$

Y- Component

$$\rho \left(\bar{u} \frac{\partial \bar{v}}{\partial x} + \bar{v} \frac{\partial \bar{v}}{\partial y} + \bar{w} \frac{\partial \bar{v}}{\partial z} \right) = -\frac{\partial \rho}{\partial y} + \mu \nabla^2 \bar{v} - \frac{\partial}{\partial y} \rho \bar{v}'^2 - \frac{\partial}{\partial x} \rho \bar{u}' \bar{v}' - \frac{\partial}{\partial z} \rho \bar{v}' \bar{w}' \quad (3)$$

Z- Component

$$\rho \left(\bar{u} \frac{\partial \bar{w}}{\partial x} + \bar{v} \frac{\partial \bar{w}}{\partial y} + \bar{w} \frac{\partial \bar{w}}{\partial z} \right) = -\frac{\partial \rho}{\partial z} + \mu \nabla^2 \bar{w} - \frac{\partial}{\partial z} \rho \bar{w}'^2 - \frac{\partial}{\partial x} \rho \bar{u}' \bar{w}' - \frac{\partial}{\partial y} \rho \bar{v}' \bar{w}' \quad (4)$$

3.13 Energy equation

$$\rho C_p \left(\bar{u} \frac{\partial \bar{T}}{\partial x} + \bar{v} \frac{\partial \bar{T}}{\partial y} + \bar{w} \frac{\partial \bar{T}}{\partial z} \right) = \mu \nabla^2 T - \frac{\partial}{\partial x} \rho C_p \bar{u}' \bar{T}' - \frac{\partial}{\partial y} \rho C_p \bar{v}' \bar{T}' - \frac{\partial}{\partial z} \rho C_p \bar{w}' \bar{T}' \quad (5)$$

Where

$$\nabla^2 = \left(\frac{\partial^2}{\partial x^2} + \frac{\partial^2}{\partial y^2} + \frac{\partial^2}{\partial z^2} \right) \quad (6)$$

From CFD analysis, temperature, heat transfer coefficient and pressure distribution on cooling

channels surface side and hot blade surface side have been obtained. The boundary conditions employed for C3X blade were taken as mentioned in references [6–8].

3.14 Boundary conditions

Boundary conditions used for the twisted blade models (1 and 2) are given below.

- Hub diameter: 1.2 m
- Number of blades: 51
- Hot air Inlet Pressure: 350 kPa
- Hot air Inlet Temperature: 1000 K
- Hot air Outlet Static Pressure: 160 kPa
- Cold air Inlet Velocity: 30 m/s
- Cold air inlet temperature: 480 K
- Rotational speed: 6000 RPM
- The computational inlet was located as 140 mm upstream of the blade leading edge. The computational exit was located as 140 mm downstream of the blade trailing edge.
- Turbulence model used – k-ε.
- 8.3% turbulence intensity and 0.4 mm eddy length scale are given at inlet of hot air flow.
- Medium 5% turbulence intensity has been used for cold side.
- Ideal air is used as a working fluid for both side hot side as well as cold side.
- The specific heat of the air as a function of temperature is given by following Equation which is presented below.
Cp = 944.23 + 0.189×T (J/kg-K) [9]
- Fluid Solid Interface is given for both side hot side and cooling air side where fluid is coming in contact with solid blade.
- Conservative interface flux with zero thermal contact resistance is used between fluid side and solid side of the interface. Conservative interface flux means at the fluid solid interface the heat flux normal to the interface is conserved.
- Rotational periodicity has been applied on fluid-fluid interface for single blade analysis purpose.

Fig. 5 shows the steady state CFD analysis of gas turbine blade.

3.2 Transient FEA Model

Finite Element Analysis (FEA) simulation software Abaqus is used for heat transfer analysis, mechanical stress analysis, thermal stress analysis and thermo-mechanical stress analysis of the gas turbine blade. The main objectives of the current study to determine the blade metal temperature distribution, maximum mechanical stress, maximum thermal stress and maximum thermo mechanical stress distribution in the gas turbine blade. Now the result obtained from the CFD analysis, temperature, heat transfer coefficient and pressure distribution on the blade surface is mapped as a boundary condition in ABAQUS 2019 for finite element analysis.

- From steady state CFD results, the blade hot side temperature, cooling side temperature and cooling side heat transfer profiles are implemented as Thermal BCs in the transient heat transfer analysis. [2] After heat transfer analysis, temperature field is obtained on the blade surface as well as inside the blade.
- From steady state CFD result, the blade surface pressure distribution and centrifugal load are considered for transient mechanical stress analysis.
- Transient heat transfer analysis result i.e. temperature is defined as a predefined load in transient thermal stress analysis.
- For transient thermo-mechanical stress analysis, blade surface pressure distribution obtains from steady state CFD result and centrifugal load used as a boundary condition with temperature consider as a predefined load obtain from transient heat transfer analysis result.

4. CFD Result

4.1 Validation of CFD model

Predicted pressure distribution and temperature distribution at C3X blade mid span was compared with the results given in references [6, 7]. Predicted pressure distribution result on mid span C3X blade is shown in Fig. 6. Predicted temperature distribution result shown in Fig. 7. The results predicted by present analysis are closely matching with the experimental and

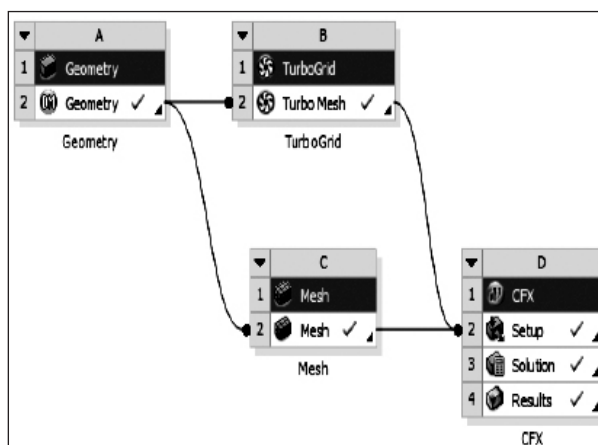


Fig. 5. Basic structure followed for steady state CFD analysis in ANSYS CFX.

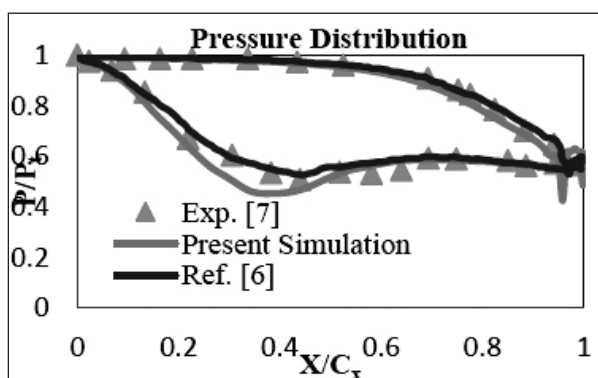


Fig. 6. Pressure distributions at mid-span of the C3X blade.

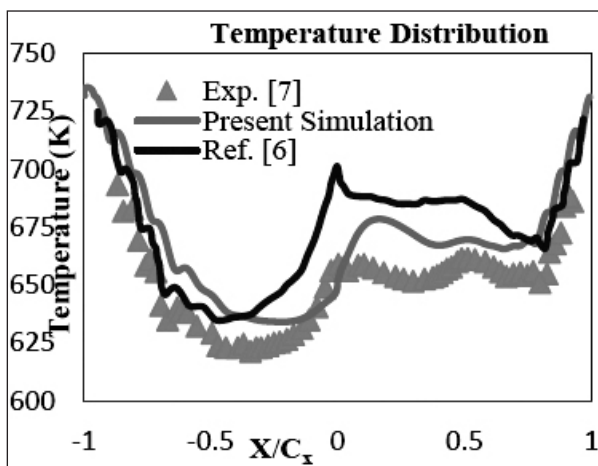


Fig. 7. Temperature distributions at mid-span of the C3X blade.

numerical data in literature. Predicted pressure distribution on mid span blade deviates from experimental and numerical results in suction side ($0 < X/C_x < 0.45$). Maximum error of 10.38% is observed at $X/C_x = 0.365$. Predicted temperature distribution on mid span of C3X blade deviates from experimental and numerical results in pressure side ($0.04 < X/C_x < 0.74$). Maximum

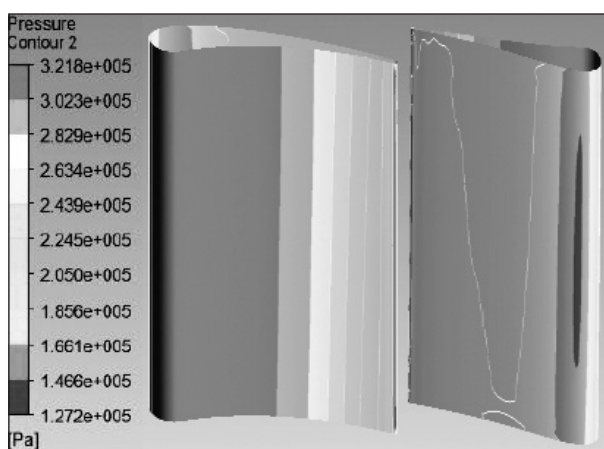


Fig. 8. Blade pressure distributions on pressure and suction side of the C3X blade.

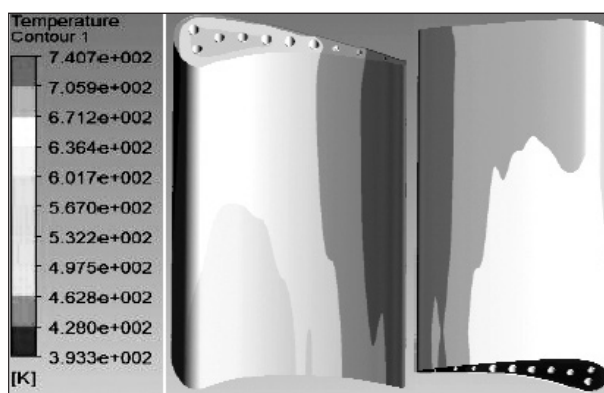


Fig. 9. Blade temperature distributions on pressure and suction side of the C3X blade.

observed error is 3.17% at $X/C_x = 0.14$. Keeping view of different method of analysis, the error in temperature distribution is acceptable. Whereas for pressure distribution although the 10.38% error at $X/C_x = 0.365$ is quite high but is quite visible that at other locations pressure distribution matches well.

The pressure distribution and temperature distribution in the C3X blade are shown in the Fig. 8 and Fig. 9 respectively. From the CFD results the maximum and minimum pressures were 321.8 kPa and 127.3 kPa respectively on the blade surface. The maximum and minimum surface temperature is 740.7 K and 393.3 K respectively.

The grid independency test is also carried out on this C3X gas turbine blade by varying the mesh size and other important parameters, till the variation of the results and nature of mid span pressure and temperature distribution is not much affected. After validation of present modelling technique, the methodology is employed of the twisted blades.

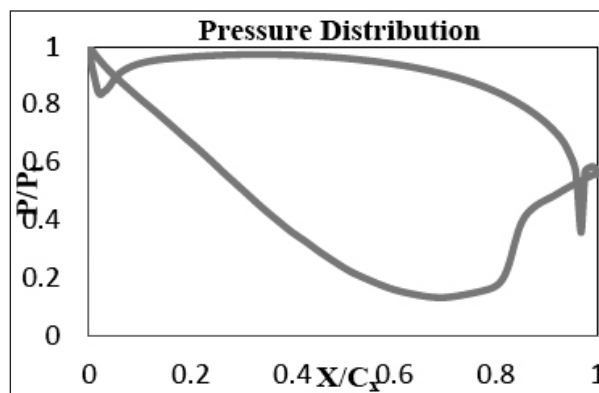


Fig. 10. Pressure distributions at mid-span of the blade surface (Model 1).

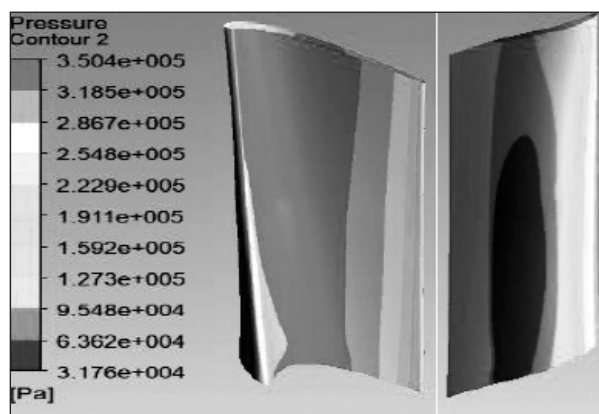


Fig. 11. Blade surface pressure distributions on pressure and suction side of the blade (Model 1).

4.2 CFD results for twisted Model 1 and Model 2

4.2.1 Model 1 (Without cooling channel)

The CFD analysis for the solid blade on ANSYS CFX provided surface temperature and pressure distribution on the blade surface. The material of the blade was used CMSX-4, which is a Ni-based single crystal superalloy. The pressure distribution and temperature distribution on the blade surface are shown in the Fig. 11 and Fig. 13 respectively. The pressure and temperature variations are plotted for the mid span of the blade surface, which is shown in the Fig. 10 and Fig. 12. From Fig. 11 the maximum and minimum pressure are 350.4 kPa and 31.76 kPa respectively on the blade surface. From Fig. 13 the maximum and minimum temperatures are 983.9 K and 949.3 K on the blade surface respectively.

Fig. 10 and Fig. 12 represents the pressure and temperature distribution at mid span of the blade similar to the distribution obtained for C3X

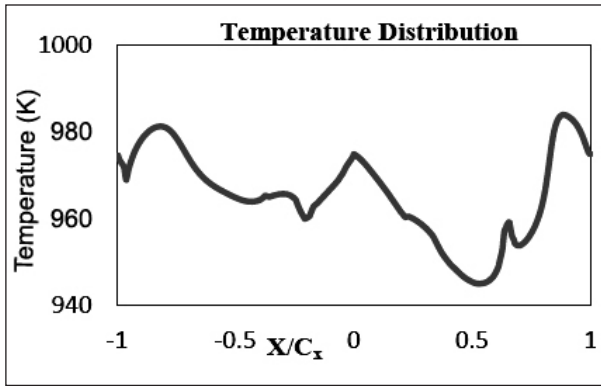


Fig. 12. Temperature distributions at the midspan of the blade surface (Model 1).

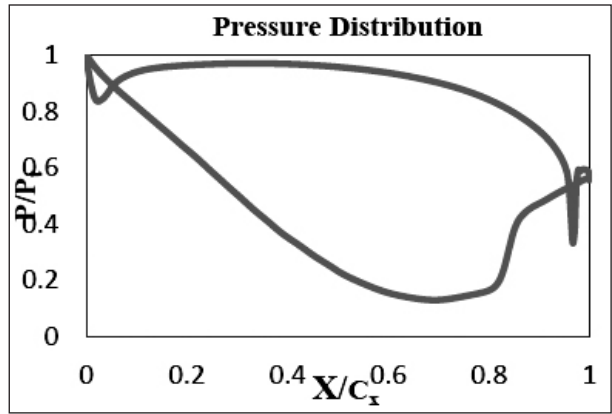


Fig. 14. Pressure distributions at mid-span of the blade surface (Model 2).

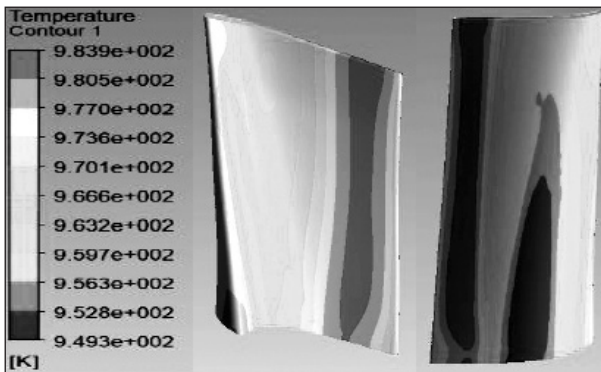


Fig. 13. Blade surface temperature distributions on pressure and suction side of the blade (Model 1).

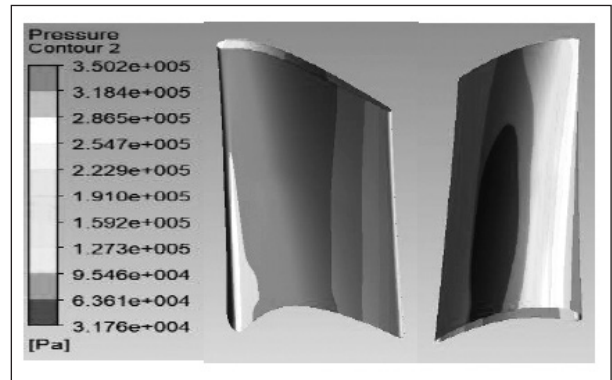


Fig. 15. Blade surface pressure distributions on pressure and suction side of the blade (Model 2).

blade (Fig. 6 and Fig. 7). It is clear that trend of distribution is almost same with few more fluctuations in the present blade without cooling holes. There is more decrease in pressure at the suction surface of the blade which is shown in Fig. 11.

4.22 Model 2 (With cooling channel)

For model 2 with cooling channel, Fig. 15 CFD Results show the maximum and minimum pressure of 350.2 kPa and 31.7 kPa respectively on the blade surface. The maximum and minimum temperatures were found as 967.5 K and 849.3 K respectively on the blade surface as shown in Fig. 17. In cooling channel maximum and minimum temperatures were 964.6 K and 849.3 K respectively on the cooling channel surface. The maximum and minimum values of heat transfer coefficient were found 1058 W/m²K and 41.13 W/m²K respectively on the cooling channel surface. The pressure distribution and temperature distribution on the blade surface are shown in the Fig. 15 and Fig. 17 respectively. The pressure and temperature variation along the mid span of the blade surface are shown in

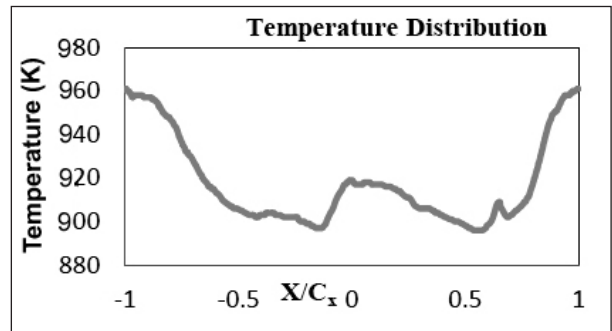


Fig. 16. Temperature distributions at the mid span of the blade surface (Model 2).

the Fig. 14 and Fig. 16. The pressure distribution along the mid span (Fig. 14) is almost same as for solid blade (Fig. 10) but there is appreciable change in temperature distribution at the mid span (Fig. 12 and Fig. 16). Cooling holes reduce the surface temperature of the blade.

5.FEA Model Result for Model 1 and Model 2

After conducting CFD analysis on both solid and cooling channel blades finite element analysis on both blades was done to determine

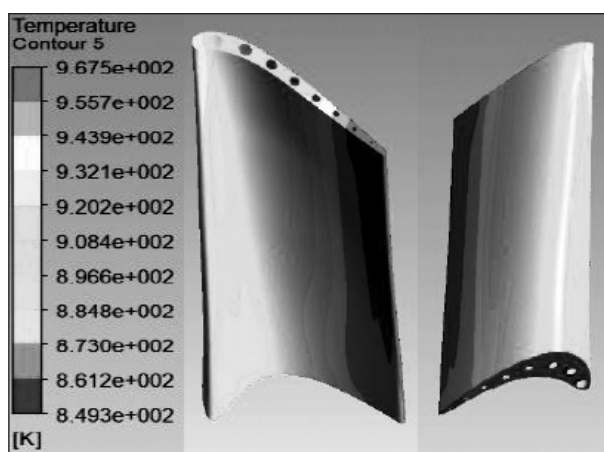


Fig. 17. Blade surface temperature distributions on pressure and suction side of the blade (Model 2).

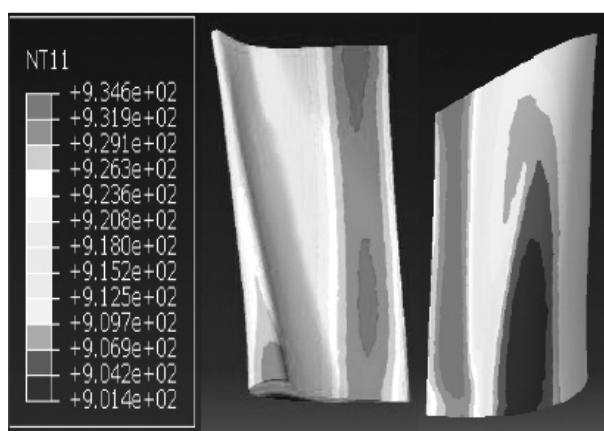


Fig. 18. Turbine blade temperature variations profile for thermal loading (Model 1).

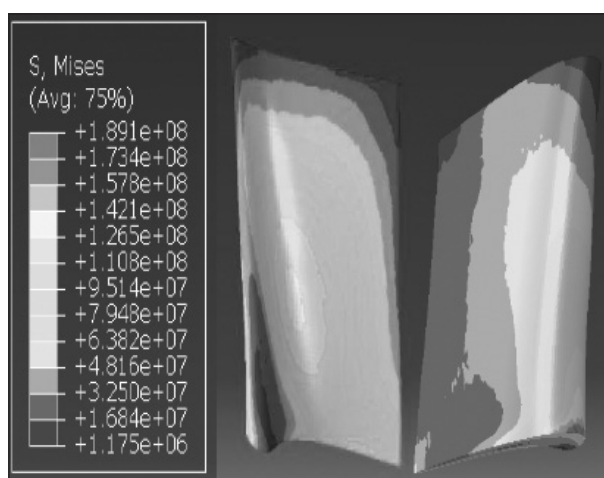


Fig. 19. Stresses in turbine blade due to centrifugal and pressure loading (Model 1).

distribution of stress, strain and temperature in both types of blades. Variable thermal and mechanical load were applied on both type of turbine blades during one cycle of 5000 second was consider on mission cycle consisting of idle, take-off, cruise, descent and landing. Different

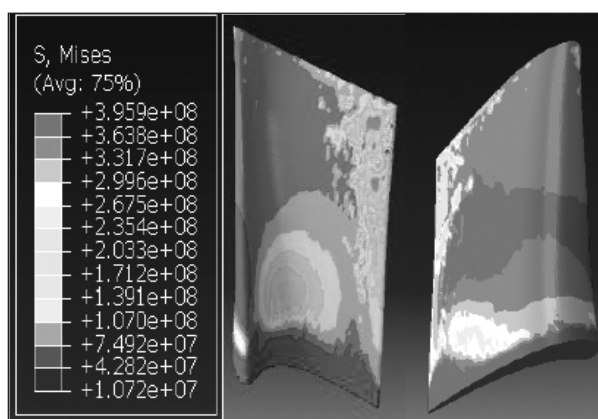


Fig. 20. Thermal stresses in turbine blade (Model 1).

results obtained for transient analysis are given in Fig. 18 to Fig. 23.

5.1 Model 1 (Without cooling channel)

5.1.1 Heat transfer analysis result

Temperature variation in blade is shown in Fig. 18 at time 4475 second. Maximum and minimum temperatures were found as 934.6 K and 901.4 K respectively.

5.1.2 Mechanical stress analysis result

Mechanical stress develops due to both centrifugal and pressure load in turbine blade. Mechanical stress distribution in the blade without cooling channels are shown in Fig. 19 at time 4658 second. Turbine blade is rotating at variable amplitude speed during one cycle (one mission cycle). The maximum and minimum Von-Misses stresses are 189.1 MPa and 1.17 MPa respectively. Maximum stress is developed in suction side hub surface of the blade.

5.1.3 Thermal stress analysis result

Thermal stress develops due to predefine temperature field from heat transfer analysis of turbine blade obtained from FE analysis present in Fig. 20. The maximum and minimum thermal stresses were found as 395.9 MPa and 10.72 MPa respectively.

5.1.4 Thermo-mechanical stress analysis result

Thermo-mechanical stress develops due to both centrifugal and pressure load along with predefined temperature field from heat transfer analysis of turbine blade. Thermo - mechanical stress is shown in Fig. 21 at time

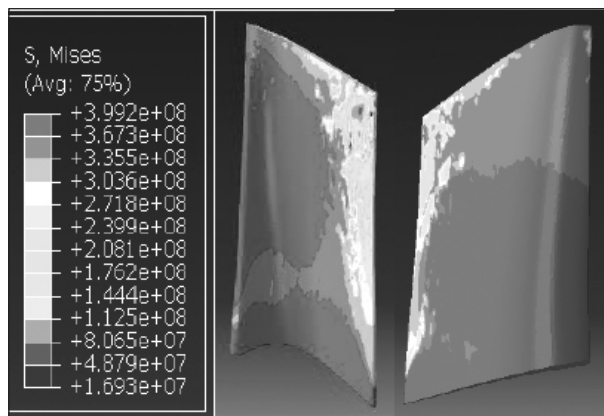


Fig. 21. Thermo-mechanical stresses in turbine blade (Model 1).

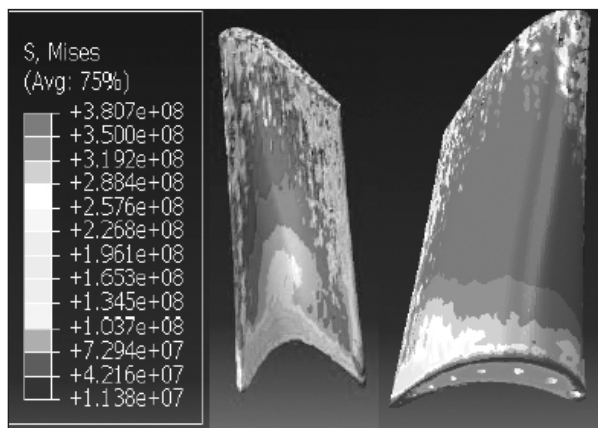


Fig. 24. Thermal stresses in turbine blade (Model 2).

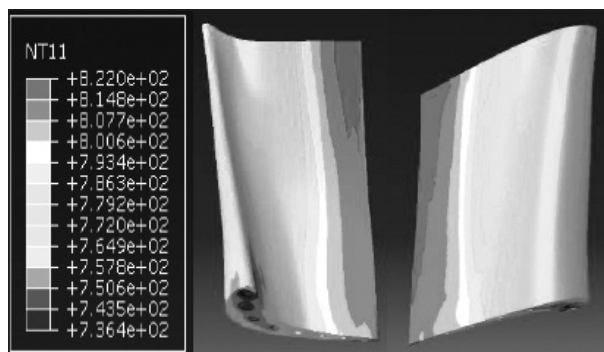


Fig. 22. Turbine blade temperature variations profile for thermal loading (Model 2).

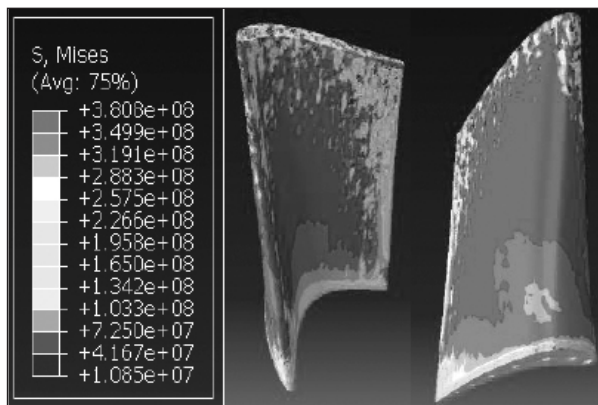


Fig. 25. Thermo-mechanical stresses in turbine blade (Model 2).

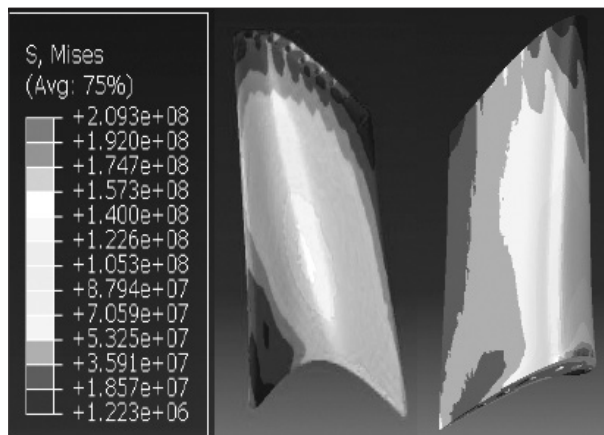


Fig. 23. Stresses in turbine blade due to centrifugal and pressure loading (Model 2).

614.3 second. The maximum and minimum thermo-mechanical stresses are 399.2 MPa and 16.93 MPa respectively.

5.2 Model 2 (With cooling channel)

5.2.1 Heat transfer analysis result

Temperature variation in blade is shown in Fig. 22 at time 481 second. Maximum and

minimum temperatures were found as 822 K and 736.4 K respectively.

5.2.2 Mechanical stress analysis result

Mechanical stress develops due to both centrifugal and pressure load in turbine blade. Mechanical stress distribution in the blade without cooling channels are shown in Fig. 23 at time 4391 second. Turbine blade is rotating at variable amplitude speed during one cycle (one mission cycle). The maximum and minimum Von-Misses stresses is 203.3 MPa and 1.223 MPa. Maximum stress is developed in suction side hub surface of the blade.

5.2.3 Thermal stress analysis result

Thermal stress develops due to predefine temperature field from heat transfer analysis of turbine blade obtained from FE analysis present in this section. Thermal stresses distribution in blade is shown in Fig. 24 at time 5000 second. The maximum and minimum thermal stresses were found as 280.7 MPa and 11.38 MPa respectively.

5.24 Thermo-mechanical stress analysis result

Thermo-mechanical stress develops due to both centrifugal and pressure load along with predefined temperature field from heat transfer analysis of turbine blade. Thermo-mechanical stress, distributions in blade is shown in Fig. 25 at time 614.3 second. The maximum and minimum thermo-mechanical stresses are 380.8 MPa and 10.85 MPa respectively.

6. Conclusion

- From the CFD analysis it was found that the maximum temperature in the blade surfaced is highest for the Model 1 in the trailing edge side where no cooling is provided. Maximum and minimum temperatures for Model 2 were less as compared to Model 1 and were 64 K and 100 K respectively.
- After performing transient heat transfer analysis maximum temperature for Model 1 and Model 2 was 944.6 K at time 510.1 second and 928.3 K at time 624.6 second respectively.
- Maximum mechanical stress and strain was found at suction surface near the hub section and maximum displacement was found in trailing area of the shroud section.
- In transient thermo-mechanical analysis, maximum stress for Model 1 and Model 2 was 399.2 MPa at time 614.3 second and 380.8 MPa at time 614.3 second respectively.

References

1. Abu, A.O., Samir, E., Laskaridis, P., & Riti, S. (2014). Aero-engine turbine blade life assessment using the Neu/Sehitoglu damage model. *International Journal of Fatigue*, 61, 160–169. 10.1016/j.ijfatigue.2014.11.015.
2. Wilson, D.G. (1984). *Design of High-Efficiency Turbo machinery and Gas Turbines* (1st ed). MIT Press.
3. Eggart, J., & Thompson, C.E. (2014). *Heavy Duty Gas Turbine Operating and Maintenance Considerations*. GE Gas Turbine.
4. Abu A.O., (2013). *Integrated approach for stress based lifting of aero gas turbine blades*. Cranfield University.
5. Zhuang, W.Z., & Swansson, N.S. (1998). *Thermo-mechanical fatigue life prediction: A critical*

review (DSTO-TR-0609). DSTO Aeronautical Maritime Research Laboratory.

6. Luo, J., & Razinsky, E.H. (2007). Conjugate Heat Transfer Analysis of a Cooled Turbine Vane Using the V2F Turbulence Model. *Journal of Turbomachinery*, 129(4), 773-781.
7. Hylton, L.D., Mihelc M.S., Turner E.R., Nealy, D.A., & York, R.E. (1983). *Analytical and Experimental Evaluation of the Heat Transfer Distribution Over the Surfaces of Turbine Vanes* (19830020105). NASA Lewis Research Center.
8. Reyhani, M.R., Alizadeh, M., Fathi, A., & Khaledi, H. (2013). Turbine blade temperature calculation and life estimation - a sensitivity analysis. *Propulsion and Power Research*, 2(2), 148–161.
9. Cengel, Y.A., & Cimbala, J.M., *Refrigeration and Air conditioning. McGraw-Hill Series in Mechanical Engineering*.



Mr. Ganesh, Research fellow, Mechanical Engineering Department, Motilal Nehru National Institute of Technology Allahabad, Prayagraj U.P (India). He has completed his M.Tech from NIT Hamirpur H. P (India) in CAD-CAM from Mechanical Engineering Department in 2018. After it He had worked as a research fellow in Mechanical Engineering Department in MNNIT Allahabad, Prayagraj U. P (INDIA). His area of research is in aerospace. He has experience for one year and four months in Project implementation of life prediction of gas turbine blade. He knows to work on Analytical and Design Software such as Ansys CFX, Catia, CFD, ABAQUS and FE-safe. He has published 4 international conference paper related to aerospace area.

Prof. (Dr.) K. N. Pandey, Professor, Mechanical Engineering Department, Motilal Nehru National Institute of Technology Allahabad, Prayagraj U.P (India). He obtained Ph.D. from University of Allahabad. He has more than 25 years of Teaching, Industrial and Research experience. He published over 40 technical and research papers in various international and national journals and conferences. He has guided 4 Ph.Ds. He has organized 5 workshops, 20 international conferences and delivered 25 keynote and invited talks. His area of interest is in Fatigue and Fracture and Tribology.



Mr. Devendra Pratap Singh Received his B. Tech Degree from a Semi Government College U.P (INDIA) in Mechanical Engineering. He has completed his M.Tech from MNNIT Allahabad U.P (India) in CAD-CAM from Mechanical Engineering Department in 2019. His area of research is in Gas Turbine. He knows to work on Analytical and Design Software such as Ansys CFX, Catia, CFD, ABAQUS and FE-safe. He has published 1 international conference paper related to aerospace area.